Interaction between magnetic domain walls and antiphase boundaries in Ni2Mn(Al,Ga) studied by electron holography and Lorentz Microscopy

Materials Transactions, Vol. 48, No. 10 (2007) pp. 2636 to 2641
Special Issue on Advances in Electron Microscopy for Materials Characterization

Interaction between Magnetic Domain Walls and Antiphase Boundaries in $Ni_2Mn(Al,Ga)$ Studied by Electron Holography and Lorentz Microscopy

T. Yano[1,*], Y. Murakami[1], R. Kainuma[1,2] and D. Shindo[1]

[1]*Institute of Multidisciplinary Research for Advanced Materials, Tohoku University, Sendai 980-8577, Japan*
[2]*CREST-JST, Tokyo 105-6218, Japan*

The magnetization distribution in the $L2_1$ phase of a $Ni_2Mn(Al,Ga)$ alloy, which is a type of ferromagnetic shape memory alloy, has been studied by electron holography and Lorentz microscopy. This alloy contains many antiphase boundaries (APBs), which are introduced by the chemical ordering from the B2 state to the $L2_1$ state. *In situ* Lorentz microscopy observations have revealed that APBs behave as strong pinning sites for domain wall motion. The width of a 180° wall, which was formed at the position of an APB, was estimated to be approximately 10 nm. This narrow domain wall was rationalized by the depression of ferromagnetism within APBs. [doi:10.2320/matertrans.MD200783]

(Received June 28, 2007; Accepted July 31, 2007; Published September 25, 2007)

Keywords: *antiphase boundary, ferromagnetic shape memory alloy, Lorentz microscopy, electron holography, magnetic domains*

1. Introduction

Ferromagnetic shape memory alloys (FMSMAs) have attracted considerable attention from many researchers due to their potential applications to actuators, which can be driven by an applied magnetic field. The anomalously large magnetostriction, which reaches magnitudes of the order of 10^{-2}, originates from the twinning deformation induced by the magnetic field. As first reported by Ullakko and his collaborators,[1)] the large magnetocrystalline anisotropy of martensite (low-temperature phase) is the most important factor in achieving magnetic-field-induced twinning deformation.

Many FMSMAs—Ni_2MnGa,[1,2)] Ni_2MnAl,[3)] Ni_2MnIn,[4,5)] Ni_2MnSn,[4,6)] Ni_2FeGa[7)] etc.—have an $L2_1$ ordered structure in the parent phase (high-temperature phase). Therefore, this phase contains antiphase boundaries (APBs) that are formed by the chemical ordering from the B2 state to the $L2_1$ state. The APBs formed by a thermal reaction have a finite width, which reaches several nanometers or larger depending on the conditions of heat treatment.[8,9)] Consequently, the magnetic moment can be small near the APBs when the magnetism strongly depends on the degree of chemical order. Because of this local modulation of magnetism, APBs are regarded as an important factor in the control of magnetic properties in ordered alloys. In fact, it was reported that APBs affect significantly the magnetization process in several alloys of hard magnets.[10–13)] Thus, it is also important to examine the effect of APBs on the magnetic properties and/or magnetic domain structures in FMSMAs; this is the motivation of the present study.

Several researchers have mentioned the role of APBs in FMSMAs. Oikawa *et al.*[7)] claimed to have observed an anomalous temperature dependence of the thermomagnetization curve of a $Ni_{51}Fe_{22}Ga_{27}$ alloy, in which the observable magnetization in the parent phase is reduced with an approach to Ms (martensitic transformation start temperature). This phenomenon is due to the pronounced interaction between the magnetic domain walls and the APBs, as revealed by *in situ* observations using Lorentz microscopy and electron holography.[14,15)] The significant interaction between the magnetic domain walls and the APBs was also observed in a Ni_2MnGa alloy system.[16)] More recently, some of the present authors[17)] carried out transmission electron microscopy (TEM) studies on $Ni_2Mn(Al,Ga)$ alloys, which belong to a class of FMSMAs. With respect to the crystal structure, the $Ni_2Mn(Al,Ga)$ alloy is regarded as being similar to the Ni_2MnGa system with Al substituted for Ga. Although the conventional dark-field imaging of APBs is difficult in Ni_2MnGa alloys in which the atomic numbers of Mn and Ga are close to each other,[16)] the substitution of Al for Ga makes the imaging easier. Another important feature of the $Ni_2Mn(Al,Ga)$ alloy is that the magnetic order strongly depends on the chemical order. In fact, the $Ni_2Mn(Al,Ga)$ alloy is ferromagnetic in the $L2_1$ ordered state, while it is antiferromagnetic in the disordered B2 state.[18)] This fact implies that the interaction between the magnetic domain walls and the APBs is more significant compared with other systems (e.g. $Ni_{51}Fe_{22}Ga_{27}$) that continue to exhibit ferromagnetism in the B2 state. Thus, the $Ni_2Mn(Al,Ga)$ alloy appears to be an ideal system to study the role of APBs on the magnetic domains. Actually, the magnetic domain walls are affected by the positions of APBs in the parent phase of the $Ni_2Mn(Al,Ga)$ alloy, and their correlation is also apparent in the martensite, whose magnetocrystalline anisotropy is larger by two orders of magnitude as compared to that of the parent phase.[19)] These observations predict a significant pinning effect of APBs on magnetic domain walls. In order to confirm the prediction of the pinning effect, the magnetization process should be observed *in situ* by transmission electron microscopy. Moreover, in order to further understand the significant interaction, it will be beneficial to evaluate the width of magnetic domain walls that are trapped by APBs.

The purpose of the present work is to examine the interaction between APBs and magnetic domain walls in the parent phase of a $Ni_2Mn(Al,Ga)$ alloy by electron holography and Lorentz microscopy. In particular, we focus on (1) domain wall pinning by APBs and (2) the width of the magnetic domain walls that are trapped by APBs.

*Corresponding author, E-mail: yano@mail.tagen.tohoku.ac.jp

2. Experimental Procedure

An ingot having a stoichiometric composition $Ni_{50}Mn_{25}Al_{12.5}Ga_{12.5}$ was fabricated by induction melting. For homogenization, the ingot was annealed at 1273 K for 3 days and quenched in ice water. In order to develop the $L2_1$ ordered structure and increase the size of the antiphase domains (APDs) to the order of 100 nm, the ingot was heated to 1073 K and then slowly cooled to 673 K in 1 day; this was followed by quenching in ice water. For the TEM studies, thin foil specimens were prepared by electrochemical polishing.

APBs were observed by using the transmission electron microscopes JEM-2000EX and JEM-2010Ω, and the latter had an omega-type energy filter[20] attached to it. The magnetic domain structure was studied by using a transmission electron microscope, JEM-3000F, in which a magnetically shielded objective lens and an electron biprism were installed.[21] The magnetic field at the specimen position was reduced to 0.04 mT due to the shielding. The position of the magnetic domain walls was determined by the Fresnel mode of Lorentz microscopy,[20,22] by which the domain walls could be clearly imaged as bright lines and dark lines. In order to reveal the magnetization distribution near the APBs, we employed electron holography;[20,23] this technique enables the lines of magnetic flux to be clearly imaged, as shown in a later section. In order to carry out *in situ* observations of the magnetization process, a special specimen holder (magnetizing stage) equipped with a small electromagnet was used.[24]

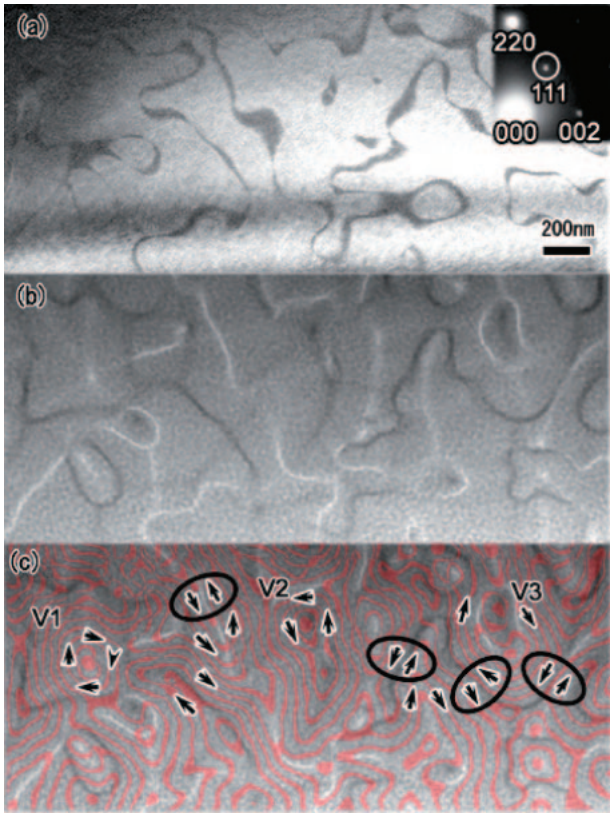

Fig. 1 (a) Dark-field image showing APBs in the parent phase of $Ni_{50}Mn_{25}Al_{12.5}Ga_{12.5}$. (b) Lorentz microscope image in the same area of (a). (c) Reconstructed phase image superposed on the Lorentz microscope image. Red lines and black arrows in (c) represent the lines of magnetic flux and their directions, respectively.

3. Results and Discussion

Figure 1(a) shows a dark-field image of the parent phase of the $Ni_{50}Mn_{25}Al_{12.5}Ga_{12.5}$ alloy. This image was obtained by using the 111 superlattice spot, which is indicated by the white circle in the inset of the figure. The winding dark regions represent the APBs. The size of the APDs ranges from 200 nm to 500 nm. Figure 1(b) depicts a Lorentz micrograph that is observed in the same field of view as that shown in Fig. 1(a). The magnetic domain walls are visualized as bright and dark lines. Most of the magnetic domain walls are placed at the positions of the APBs, although they are also present at some positions other than APBs, as described later in detail. Figure 1(c) shows a reconstructed phase image (obtained from electron holography) superposed on the Lorentz micrograph in Fig. 1(b). The red contour lines in Fig. 1(c) represent the in-plane component of the magnetic flux. The black arrows indicate the direction of the magnetic flux. The direction of magnetic flux steeply changes near the APBs. In fact, at several APB positions, the flux lines rotate by approximately 180° (refer to the circled portions in Fig. 1(c)). The magnetic flux exists as a vortex inside a closed and/or heavily curved APB (refer to the vortices V1, V2, and V3) as reported by the previous work.[19] These configurations are a result of the strong interaction between the APBs and the magnetic domain walls.

The observations in Fig. 1 indicate that the magnetic domain walls are stabilized at the positions of APBs; therefore, a pinning effect on the domain wall motion is expected. In order to examine the pinning effect, a weak magnetic field was applied to the specimen inside the electron microscope, and the change in the domain structure was observed *in situ*. Figure 2 shows the magnetization process in the $Ni_{50}Mn_{25}Al_{12.5}Ga_{12.5}$ alloy that is in the parent phase. A magnetic field, which is approximately parallel to the foil plane, was applied by using a magnetizing stage.[24] Figure 2(a) shows a Lorentz micrograph in the parent phase in the absence of an applied magnetic field. In Fig. 2(b), the lines of magnetic flux determined by electron holography are superposed on the Lorentz micrograph of Fig. 2(a). The observed area is identical to that shown in Fig. 1(a). As mentioned earlier, the locations of most of the domain walls correspond to the position of the APBs. It is noted that a few domain walls are formed at positions not corresponding to APBs. For example, as evident from a comparison with Fig. 1(a), no APB is present at the position of the magnetic domain wall that is marked by the blue arrowhead (W1). The red arrowheads (V1 and V2) indicate the core of magnetic vortices, which are surrounded by closed and/or heavily curved APBs. When a magnetic field of 3680 A/m is applied (along a white arrow), as shown in Figs. 2(c) and 2(d), the positions of V1 and V2 are slightly shifted downward. This motion occurs due to the increase in the volume fraction of magnetization vectors that are parallel to the applied magnetic field. Due to the same reason, it is likely that the

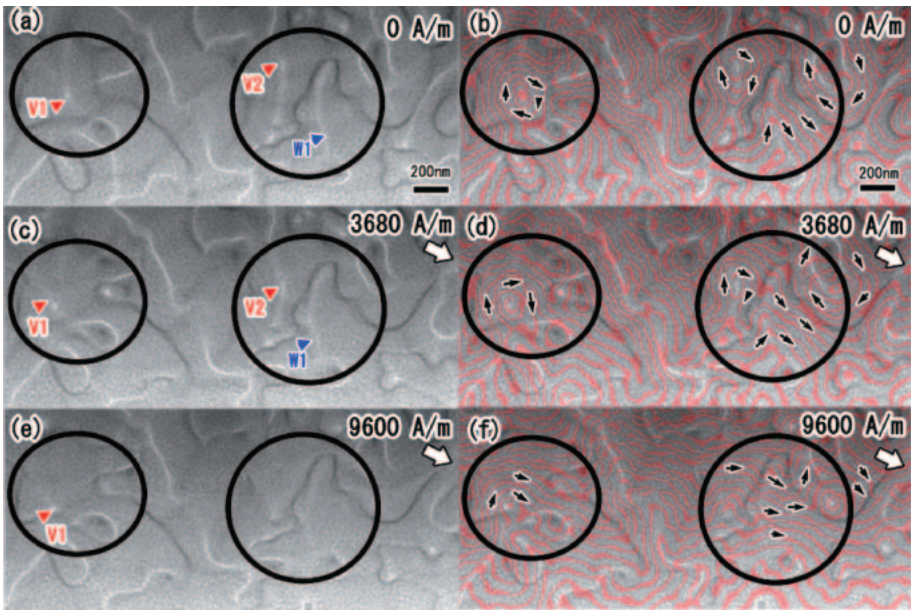

Fig. 2 Magnetization process of a $Ni_{50}Mn_{25}Al_{12.5}Ga_{12.5}$ alloy. (a), (c), (e) Changes in the Lorentz microscope images with application of magnetic fields. (b), (d), (f) Changes in the reconstructed phase images with the applied magnetic fields. The reconstructed phase images are superposed on the Lorentz microscope images of (a), (c), (e). White arrows indicate the direction of applied magnetic fields.

domain wall contrast at W1 becomes obscured. However, in the weak magnetic field of 3680 A/m, the magnetic domain walls trapped by APBs do not shift. In a larger magnetic field of 9600 A/m, vortex core V2 and domain wall W1 disappear, as shown in Fig. 2(e) and 2(f). However, the lines of magnetic flux continue to have a winding form at the positions of APBs (refer to Fig. 2(f)). In fact, magnetic domain walls are still visible near APBs, as shown in the Lorentz micrograph of Fig. 2(e). Unfortunately, the application of a larger magnetic field degraded the visibility of electron holograms; therefore, a magnetic flux map could not be obtained in a magnetic field greater than 9600 A/m. Nevertheless, the observations demonstrate that magnetic domain walls are stabilized at the positions of APBs. It is noted that the values of the applied magnetic field (3680 A/m and 9600 A/m) are nominal ones that are estimated from the coil current in the electromagnet.[24] Due to the inhomogeneous magnetic field distribution in the magnetizing stage, the actual magnetic field at the observed portion may be smaller than those nominal values. Despite the fact, it is possible to discuss the magnetization process with increase of the magnetic field by using this technique.

The magnetization process was also recoded by using a TV camera in order to understand the dynamics of domain wall motion in greater detail. When a magnetic field is applied, the magnetization distribution first changes in the areas that are distant from the APBs, *e.g.,* the motion of the vortex center (shown in Fig. 2). Subsequently, the magnetic domain walls placed at APBs move in a larger magnetic field. However, once a magnetic domain wall is released from the APB, it is immediately trapped by a nearby APB. Figure 3(a) shows a video frame of the movie recorded by the TV camera. By considering the coil current in the electromagnet, the magnetic field applied along the white arrow is estimated to be approximately 6400 A/m. Most of the magnetic domain

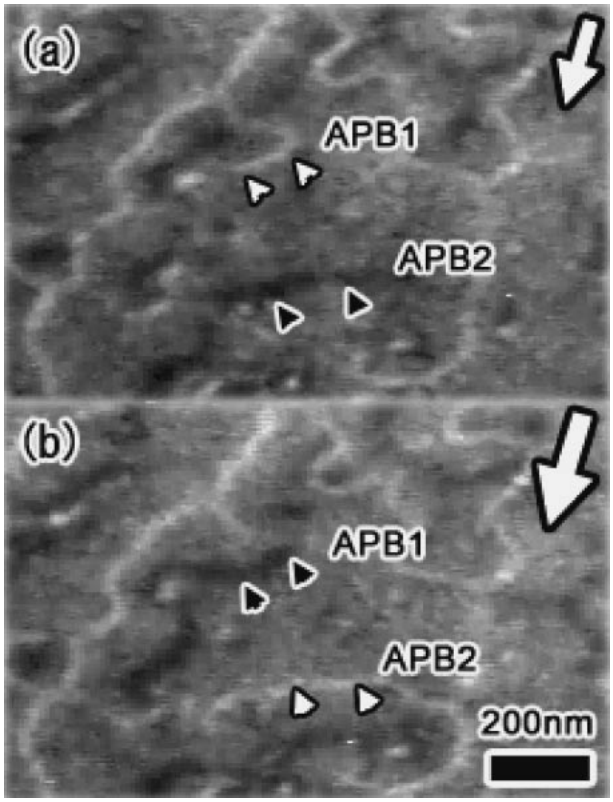

Fig. 3 Captures of video frames showing the motion of magnetic domain walls in the parent phase of $Ni_{50}Mn_{25}Al_{12.5}Ga_{12.5}$. The observation was performed in the Fresnel mode of Lorentz microscopy. Magnetic domain walls are placed at the positions of APBs in (a). By increasing the magnetic field, the domain walls are released from the APBs, but the domain walls are soon trapped by nearby APBs as shown in (b). One frame corresponds to 1/30 s in the video rate. White arrows indicate the direction of applied magnetic fields.

walls (bright and dark lines) are placed at the positions of APBs in Fig. 3(a). For example, a bright line is observed at the position of "APB1," while a dark line is placed at another position, "APB2." With a further increase in the magnetic field, these domain walls are released from the APBs; however, they were immediately trapped by other APBs. In fact, at the stage shown in Fig. 3(b) in which the applied magnetic field is larger than that shown in Fig. 3(a), the domain wall contrast at positions "APB1" and "APB2" has been reversed as a result of the domain wall motion. Thus, in the presence of APBs, the domain wall motion occurs intermittently rather than continuously. This observation demonstrates the significant pinning effect of APBs. Although we were unable to correctly evaluate the magnitude of the applied magnetic field due to the same reasons as mentioned earlier, the applied field in Fig. 3(b) is presumably over 8000 A/m as far as the coil current is considered. The estimation is consistent with the result of the B-H curve observed for a bulk specimen in which the coercive force is approximately 7200 A/m in the parent phase. (In Fig. 2, magnetic domain walls trapped by APBs did not move in the nominal magnetic field of 9600 A/m —presumably, the magnetic field is overestimated in the experiment of Fig. 2).

The width of the magnetic domain walls trapped by APBs is evaluated. The result is compared with a typical value of the wall width in cubic alloys, which have a similar magnitude of magnetocrystalline anisotropy. In order to determine the wall width, the Lorentz micrographs were acquired as a function of the defocus value Z. When the full width at half maximum (FWHM) W of the intensity profile, which is measured across a magnetic domain wall, is plotted against Z, its extrapolation to the zero-defocus position yields a good approximation of the wall width[25] (refer to Figs. 4(b) and 4(c)). As mentioned by several researchers,[26–28] the extrapolation by using large Z leads to an overestimation of the wall width. For example, Gong and Chapman[26] have mentioned that a linear approximation between Z and W can yield a satisfactory estimation for the wall width when Z is small (*e.g.*, in the order of 10^2 μm or smaller). The relation between Z and W tends to deviate from a straight line when Z is substantially large (*e.g.*, in the order of 10^3 μm or larger), although the examination by Gong and Chapman assumed a small accelerating voltage of 100 kV. Thus, we plotted only the results obtained in a small range of Z, i.e., 13 μm $\leqq Z \leqq$ 156 μm. On the other hand, when the plane of APBs and/or magnetic domain walls is tilted off the incident electrons, this plot leads to an overestimation of the width. In order to minimize this overestimation, we have chosen such a portion in which the observed APB width is narrow and it does not change greatly with a change in the specimen thickness.

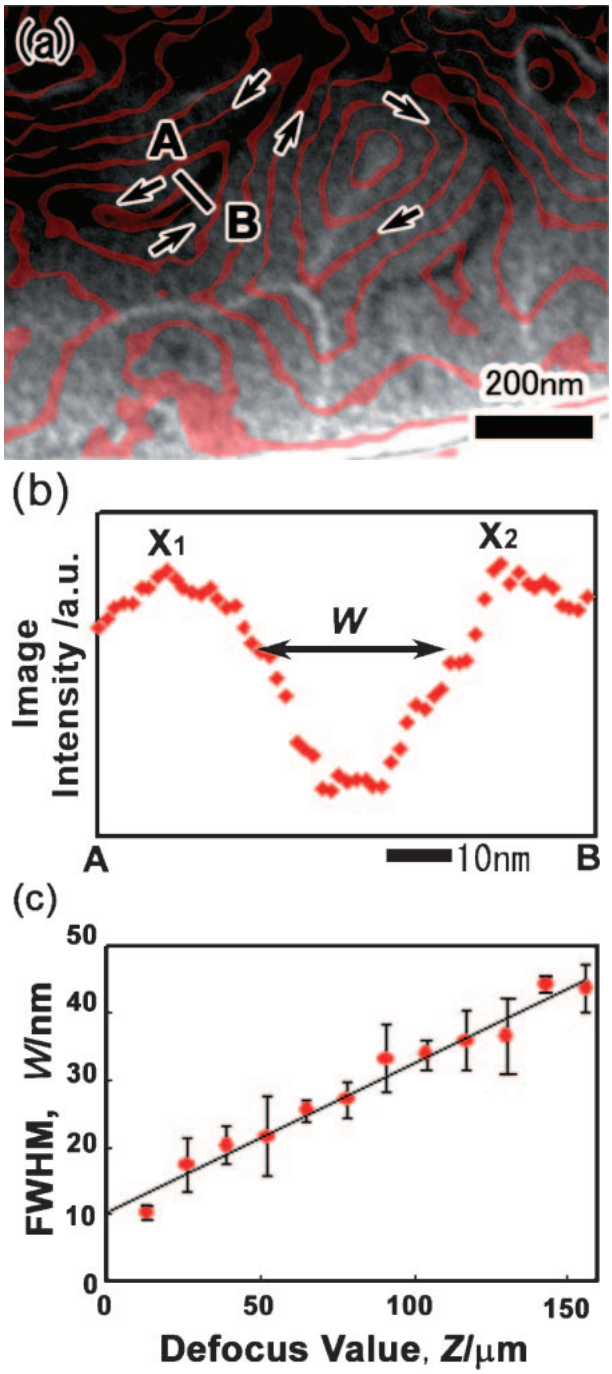

Fig. 4 (a) Lorentz microscope image in the parent phase of $Ni_{50}Mn_{25}Al_{12.5}Ga_{12.5}$. Red lines represent the lines of magnetic flux in this field of view. (b) Intensity profile that was measured across the divergent wall—refer to the line A-B across the divergent wall. (c) Full width at half maximum W of the intensity profile of the divergent wall plotted as a function of the Defocus Value Z.

The wall width was determined by using a dark contrast for the domain wall (*i.e.*, divergent wall image), as shown in Fig. 4(a); the intensity profile was obtained along the solid line A-B. The domain wall is characterized to be a 180° wall, as demonstrated by the superposed flux lines—refer to the red contour lines and black arrows which represent the lines of magnetic flux and their directions, respectively. W of the intensity profile can be determined straightforwardly, as shown in Fig. 4(b); in the intensity profile, a background is defined by a straight line that intersects the intensity maxima at X_1 and X_2. Figure 4(c) plots W as a function of Z. It is noted that the closed circles in Fig. 4(c) represent the average of W. In order to obtain this average at each condition of Z, W was measured for four points (having similar sample thickness) along the magnetic domain wall. The vertical bars offer the standard deviation, which is a measure of the accuracy of determining W. It appears that W changes linearly over the whole range of Z (13 μm $\leqq Z \leqq$ 156 μm) as far as the

accuracy of determining W is considered. By providing least-square fitting for the plots, the extrapolation to the zero-defocus position yields a wall width of 10 nm.

Apparently, the wall width determined in Fig. 4 is smaller than that of the 180° walls observed in other cubic metals and alloys. For example, the width of a 180° wall is approximately 73 nm in cubic iron.[29] In FMSMAs, the magnetic parameters A (exchange stiffness) and K (anisotropy factor) have been determined in a Ni_2MnGa alloy.[30,31] By using these magnetic parameters and the widely accepted relationship $\delta = \pi\sqrt{A/K}$, the width of a 180° wall (δ) is estimated as 67 nm in the parent phase of Ni_2MnGa when the effect of APBs is disregarded. With respect to the $Ni_2Mn(Al,Ga)$ ($Ni_{50}Mn_{25}Al_{12.5}Ga_{12.5}$) alloy in which the $L2_1$ state is achieved, Ishikawa *et al.*[18] have revealed that both the Curie temperature and saturation magnetization are comparable to those of a Ni_2MnGa alloy: the result implies that the magnetic parameters A and K of the $Ni_2Mn(Al,Ga)$ alloy are close to those of the Ni_2MnGa alloy. Thus, the observation of Fig. 4—the narrow width of 10 nm—indicates that the width of domain walls placed at APB positions is dominated by a mechanism that is distinct from that of conventional 180° walls formed in a pure ferromagnetic portion.

As mentioned earlier, the $Ni_2Mn(Al,Ga)$ alloy is ferromagnetic in the $L2_1$ ordered state, while it is antiferromagnetic in the disordered B2 state.[18] The APB is a type of structural defect, which is formed during the ordering from B2 to $L2_1$. Thus, within an APB that has a finite width,[32] the atomic order is close to the B2 state rather than the $L2_1$ state, and the magnetization is considerably small at the position of the APBs. This magnetic inhomogeneity produces a substantial amount of magnetic charges at the APBs.[33] In order to reduce the formation of magnetic charges, the magnetic domain walls (*e.g.*, 180° walls) should be placed at the position of the APBs: this charge-minimization mechanism appears to be the source of the strong interaction between the magnetic domain walls and the APBs. In the vicinity of APBs, it appears that neither the magnetic parameters nor the spin-rotation mechanism in a domain wall are identical to those in the original ferromagnetic portions. In other words, when a 180° wall is formed at the position of an APB, the magnetization rotation can be achieved in a considerably narrower space as compared to the conventional 180° walls that are formed in a pure ferromagnetic portion. With respect to the magnetic domain walls produced at APBs in the $Ni_2Mn(Al,Ga)$ alloy, it appears likely that the observed wall width is closely related with the width of APBs.

4. Conclusions

The magnetic domain structure in the $L2_1$ phase of a $Ni_2Mn(Al,Ga)$ alloy, which contains many APBs introduced by the B2→$L2_1$ ordering, was investigated by electron holography and Lorentz microscopy. The results can be summarized as follows:

(1) The APBs behave as pinning sites for the motion of magnetic domain walls. As a result, the magnetization process in the parent phase proceeds in the following sequence: (a) When a magnetic field is applied, the magnetization distribution first changes in the portions that are distant from the APBs, *e.g.*, in the pure ferromagnetic regions of the parent phase. The magnetic domain walls placed at the positions of APBs do not move at this stage. (b) In a larger magnetic field, the magnetic domain walls at the positions of APBs are released. However, the released walls are immediately trapped by nearby APBs. Thus, the domain wall motion occurs intermittently, rather than continuously.

(2) The width of the 180° walls, placed at APBs in the parent phase, has been estimated to be approximately 10 nm by Lorentz microscopy. This wall width is substantially smaller than that of 180° walls that have been reported in other cubic alloys. It is likely that the narrow 180° walls in a $Ni_2Mn(Al,Ga)$ alloy is due to the depression of ferromagnetism within the APBs, wherein the atomic order is similar to that of B2 rather than that of $L2_1$. In fact, the $Ni_2Mn(Al,Ga)$ alloy becomes antiferromagnetic in the B2 phase, while it is ferromagnetic in the $L2_1$ phase.

Acknowledgement

The authors are grateful to Professor J. N. Chapman (University of Glasgow), Messrs. H. Ishikawa and K. Kobayashi, Dr. R. Umetsu, Professors A. Fujita, K. Oikawa, and K. Ishida (Tohoku University) for useful discussions on the magnetic domain walls in this alloy. This study was partly supported by the Grant-in-Aid for Scientific Research (S) (19106002 and 18106012) and Scientific Research (C) (18560641) from Japan Society for Promotion of Science.

REFERENCES

1) K. Ullakko, J. K. Huang, C. Kanter and R. C. O'handley: Appl. Phys. Lett. **69** (1996) 1966.
2) V. A. Chernenko, E. Cesari, V. V. Kokorin and I. N. Vitenko: Scr. Metall. Mater. **33** (1995) 1239.
3) A. Fujita, K. Fukamichi, F. Gejima, R. Kainuma and K. Ishida: Appl. Phys. Lett. **77** (2000) 3054.
4) Y. Sutou, Y. Imano, N. Koeda, T. Omori, R. Kainuma, K. Ishida and K. Oikawa: Appl. Phys. Lett. **85** (2004) 4358.
5) R. Kainuma, Y. Imano, W. Ito, Y. Sutou, H. Morito, S. Okamoto, O. Kitakami, K. Oikawa, A. Fujita, T. Kanomata and K. Ishida: Nature **439** (2006) 957.
6) R. Kainuma, Y. Imano, W. Ito, H. Morito, Y. Sutou, K. Oikawa, A. Fujita, K. Ishida, S. Okamoto and T. Kanomata: Appl. Phy. Lett. **88** (2006) 192513.
7) K. Oikawa, T. Ota, T. Ohmori, Y. Tanaka, H. Morito, A. Fujita, R. Kainuma, K. Ishida and K. Fukamichi: Appl. Phys. Lett. **81** (2002) 5201.
8) Ch. Ricolleau, A. Loiseau, F. Ducastelle and R. Caudron: Phys. Rev. Lett. **68** (1992) 3591.
9) M. Ohno and T. Mohri: Philos. Mag. **83** (2003) 315.
10) K. D. Belashchenko and V. P. Antropov: J. Magn. Magn. Mater. **253** (2002) 87.
11) K. D. Belashchenko and V. P. Antropov: J. Magn. Magn. Mater. **258–259** (2003) 244.
12) B. Y. Wong, M. Willard and D. E. Laughlin: J. Magn. Magn. Mater. **169** (1997) 178.
13) B. E. Meacham, J. E. Shield and D. J. Branagan: J. Appl. Phys. **87** (2000) 6707.
14) Y. Murakami, D. Shindo, K. Oikawa, R. Kainuma and K. Ishida: Appl. Phys. Lett. **82** (2003) 3695.
15) Y. Murakami, D. Shindo, K. Oikawa, R. Kainuma and K. Ishida: Appl. Phys. Lett. **85** (2004) 6170.
16) S. P. Venkateswaran, N. T. Nuhfer and M. De Graef: Acta. Mater. **55** (2007) 2621.

17) Y. Murakami, D. Shindo, K. Kobayashi, K. Oikawa, R. Kainuma and K. Ishida: Mater. Sci. Eng. A **438–440** (2006) 1050.
18) H. Ishikawa, R. Umetsu, K. Kobayashi, A. Fujita, R. Kainuma and K. Ishida: to be submitted to Acta Mater.
19) Y. Murakami, T. Yano, D. Shindo, R. Kainuma and T. Arima: Metall. Mater. Trans. A, in printing.
20) D. Shindo and T. Oikawa: *Analytical Electron Microscopy for Materials Science* (Springer-Verlag, Tokyo, 2002).
21) D. Shindo, Y. G. Park, Y. Murakami, Y. Gao, H. Kanekiyo and S. Hirosawa: Scr. Mater. **48** (2003) 851.
22) M. De Graef and Y. Zhu: *Magnetic Imaging and its Applications to Materials* (Academic Press, San Diego, 2001).
23) A. Tonomura: *Electron Holography* (Springer-Verlag, Berlin, 1999).
24) M. Inoue, T. Tomita, M. Naruse, Z. Akase, Y. Murakami and D. Shindo: J. Electron Microsc. **54** (2005) 509.
25) V. V. Volkov and Y. Zhu: J. Appl. Phys. **85** (1999) 3254.
26) H. Gong and J. N. Chapman: J. Magn. Magn. Mater. **67** (1987) 4.
27) J. N. Chapman, E. M. Waddell, P. E. Batson and R. P. Ferrier: Ultramicroscopy **4** (1979) 283.
28) S. Tsukahara and H. Kawakatsu: J. Magn. Magn. Mater. **36** (1983) 98.
29) B. A. Lilley: Phil. Mag. **41** (1950) 792.
30) F. Albertini, L. Pareti, A. Paoluzi, L. Morellon, P. A. Algarabel, M. R. Ibarra and L. Righi: Appl. Phys. Lett. **81** (2002) 4032.
31) U. Stuhr, P. Vorderwisch and V. V. Kokorin: Phys. B **234–236** (1997) 135.
32) Although the method of evaluating the magnetic domain wall may be established, as demonstrated in Fig. 4, it is uneasy to determine accurately the width of thermally formed APBs by experiments. However, the direct measurement of APB width is an important issue which we intend to challenge in the future.
33) A. Hubert and R. Schäfer: *Magnetic Domains* (Springer-Verlag, Berlin, 1998).